An EFISH, Theoretical, and PGSE NMR Investigation on the Relevant Role of Aggregation on the Second Order Response in $CHCl_3$ of the Push−Pull Chromophores [5-[[4′-(Dimethylamino)phenyl]ethynyl]-15-[(4″-nitrophenyl)ethynyl]-10,20-diphenylporphyrinate] M(II) (M = Zn, Ni)

Maddalena Pizzotti,* Francesca Tessore, Alessio Orbelli Biroli, and Renato Ugo

Dipartimento di Chimica Inorganica Metallorganica e Analitica "L. Malatesta" dell'Università di Milano, Unità di Ricerca dell' INSTM e Istituto di Scienze e Tecnologie Molecolari del CNR (ISTM), Via G.Venezian 21, 20133 Milano, Italy

Filippo De Angelis, Simona Fantacci, and Antonio Sgamellotti

Istituto di Scienze e Tecnologie Molecolari del CNR (ISTM-CNR), c/o Dipartimento di Chimica, Via Elce di Sotto 8, 06123 Perugia, Italy

Daniele Zuccaccia and Alceo Macchioni

Dipartimento di Chimica, Università di Perugia, Via Elce di Sotto 8, 06123 Perugia, Italy

Received: March 2, 2009; Revised Manuscript Received: May 6, 2009

This work has produced experimental and theoretical evidence for the independence, on the nature of the metal, of the second order NLO response of [5-[[4′-(dimethylamino)phenyl]ethynyl]-15-[(4″-nitrophenyl)-ethynyl]-10,20-diphenylporphyrinate]M(II) NLO chromophores (M = Zn, Ni). EFISH measurements, carried out at a nonresonant 1.907 μm incident wavelength and at variable concentrations in $CHCl_3$ or in a polar and donor solvent such as DMF or by addition of an excess of pyridine to a $CHCl_3$ solution, have shown, together with a PGSE NMR investigation, that the different second order NLO response obtained in $CHCl_3$ for Zn(II) and Ni(II) NLO chromophores is due to a different aggregation in $CHCl_3$ solution. Theoretical DFT/TDDFT calculations on the NLO properties of dimeric aggregates of the NLO chromophores containing the Zn(II) center have suggested, in agreement with EFISH measurements and PGSE NMR investigation, a J aggregation which induces a doubling of the second order NLO response. The PGSE NMR investigation has also suggested a much weaker dipolar interaction for the dimerization process of the NLO chromophores containing the Ni(II) center. In this latter case the antiparallel alignment of the dipole moments of the two chromophores produces a lower second order NLO response, as experimentally observed in $CHCl_3$ solution by increasing concentration.

1. Introduction

In the last two decades a large series of investigations has been devoted to the search for organic molecules characterized by a significant second order nonlinear optical (NLO) response as building blocks for nanostructured materials with electrooptical properties.[1] The structural features necessary to produce a significant second order NLO response at the molecular level are now quite well-known; many organic and more recently organometallic push−pull NLO chromophores have been synthesized and investigated.[2]

Therien and co-workers[3] reported the synthesis and second order NLO response of a new, interesting class of push−pull chromophores based on 5-X-15-Y-10,20-diphenylporphyrine and its Zn(II) (**1**) and Cu(II) (**2**) complexes (X = 4-$Me_2NC_6H_4C{\equiv}C-$; Y = 4-$NO_2C_6H_4C{\equiv}C-$) (Figure 1). For these second order NLO chromophores, an exceptionally large quadratic hyperpolarizability ($\beta_{1.064} = 4933 \times 10^{-30}$ esu for **1** and 1501×10^{-30} esu for **2**, respectively) was measured by using the hyper-Raleigh scattering (HRS) technique,[4] but working with a resonant incident wavelength of 1.064 μm.

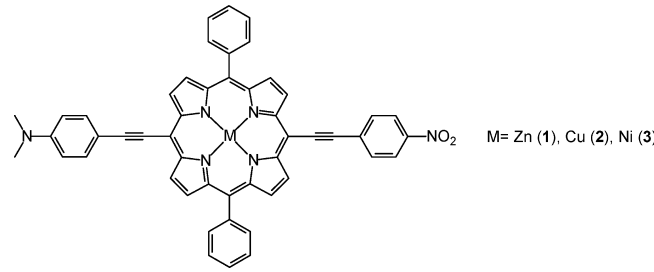

Figure 1. NLO chromophores investigated in this work.

In a second time, the value of $\beta_{1.064}$ of **1**, obtained by an investigation based on the Stark effect, was reported to be lower but still very high ($\beta_{1.064} = 1710 \times 10^{-30}$ esu).[5]

However, for some structurally related push−pull Ni(II) porphyrinic chromophores (X = 4-$Me_2NC_6H_4C{\equiv}C$, Y = CHO, $-CH{=}C(CN)_2$, $-CH{=}C(CO_2Et)_2$),[6] and for the Ni(II) complex **3**,[7] analogous to **1** and **2**, much lower values of the quadratic hyperpolarizability ($\beta_{1.907}$ about $80-120 \times 10^{-30}$ esu) were measured by the EFISH technique (Electric Field Induced

* To whom correspondence should be addressed. E-mail: maddalena.pizzotti@unimi.it.

10.1021/jp901919u CCC: $40.75
Published on Web 06/03/2009

Second Harmonic Generation)[8] but working with a nonresonant incident wavelength of 1.907 μm. Such a striking difference of the order of magnitude of the quadratic hyperpolarizability of this kind of NLO chromophores has suggested that the specificity of different experimental techniques and in particular the role of the incident wavelength (resonant or nonresonant) should be taken into careful consideration when comparing the various experimental data. Moreover, the nature of the metal could strongly influence the second order NLO response of this kind of porphyrinic push−pull chromophores.[7]

Recently some of us carried out a theoretical investigation in order to produce, by time dependent (TD) Hartree−Fock (HF) and density functional theory (DFT) calculations, information on the electronic origin of the linear and nonlinear optical properties of the NLO chromophores **1**, **2**, and **3**.[9] Coupled perturbed-DFT (CP-DFT) and coupled perturbed-HF (CP-HF) calculations provided similar and relatively low values of the quadratic hyperpolarizability of the three NLO chromophores **1**, **2**, and **3**, if compared to the large experimental values reported for **1** and **2**,[3,5] thus suggesting an irrelevant role of the metal.

In order to clarify the origin of such a striking difference, we have carried out an EFISH experimental investigation on **1** and **3**, working with a nonresonant incident wavelength of 1.907 μm, in solvents of different dielectric constant, such as DMF, $CHCl_3$, or even $CHCl_3$, added with excess pyridine, and in the case of $CHCl_3$, in a large range of concentrations ($10^{-4}-10^{-6}$ M). By this approach, differences produced by different experimental techniques or originated from resonance enhancement of the second order NLO response can be avoided.

The extension to solvents of different dielectric constant and donor properties and, in the case of $CHCl_3$, to a large range of concentrations allowed the investigation of aggregation processes. In fact, it is known that some porphyrins and their metal complexes may aggregate, for instance by π stacking,[10] leading to H or J aggregates.[11] The H or J aggregation is often characterized by spectral shifts of some electronic absorption bands or by the appearance of new absorption bands due to excitonic interactions,[12] resulting generally in a red shift for the J aggregation and a blue shift for the H aggregation.

In this work, we report a spectroscopic and EFISH experimental investigation on the NLO chromophores **1** and **3** which show, respectively, the highest and lowest reported experimental values of the quadratic hyperpolarizability.[3,5,7] Theoretical DFT calculations of the electronic absorption spectra and CP-DFT and CP-HF calculations of the quadratic hyperpolarizabilities of the pyridine adducts and of the dimeric J aggregates of **1** and **3** are also reported, together with the results of an experimental PGSE NMR investigation, carried out in order to estimate the degree of aggregation in $CHCl_3$ solution of **1** and **3**, as further support of some evidence for aggregation produced by the EFISH investigation.

2. Experimental Section

$[Pd(PPh_3)_2Cl_2]$, CH_3CN, and THF on molecular sieves have been purchased from Fluka; CuI, NEt_3, 4-dimethylaminophenylacetylene, 4-nitrophenylacetylene, and all the solvents for chromatographic separations and for EFISH measurements have been purchased from Sigma-Aldrich. Silica gel (Kieselgel 60, 0.063−0.200 mm) and Florisil have been purchased from Merck. Immediately before use, NEt_3 has been distilled over KOH and THF has been distilled in the presence of Na/benzophenone. Reactions have been carried out in flame-dried Schlenk tubes.

Elemental analyses have been carried out in the Analytical Laboratories of the Department of Inorganic, Metallorganic and Analytical Chemistry "L. Malatesta" of Milan University.

The compounds 5-iodo-15-bromo-10,20-diphenylporphyrin,[13] [5-iodo-15-bromo-10,20-diphenylporphyrinate]Zn(II),[13] and [5-[(4′-(dimethylamino)phenyl)ethynyl]-15-[(4″-nitrophenyl)ethynyl]-10,20-diphenylporphyrinate]Ni(II) (**3**)[7] have been prepared according to the literature. ^{1}H NMR spectra have been recorded in $CDCl_3$ on Bruker DRX-300 and Bruker AVANCE DRX 400 spectrometers, and pyridine-d_5 has been used in experiments involving addition of an excess of pyridine. Electronic absorption spectra have been recorded on a JASCO V-530 spectrometer.

EFISH Measurements. EFISH measurements have been performed at the Department of Inorganic, Metallorganic and Analytical Chemistry "L. Malatesta" of Milan University, working in $CHCl_3$ (amylene stabilized), DMF, and $CHCl_3$ with addition of an excess of pyridine. The investigation in $CHCl_3$ has been carried out in a range of concentrations ($10^{-4}-10^{-6}$ M). EFISH measurements have been carried out working with a 1.907 μm incident wavelength, obtained by Raman shifting of the 1.064 μm emission of a Q-switched Nd:YAG laser in a high pressure hydrogen cell (60 bar). A liquid cell with thick windows in the wedge configuration has been used to obtain the Maker fringe pattern (harmonic intensity variation as a function of liquid cell translation).[14] In the EFISH experiments the incident beam has been synchronized with a DC field applied to the solution, with 60 and 20 ns pulse duration, respectively, in order to break its centrosymmetry. From the concentration dependence of the harmonic signal compared with that of the pure solvent, the second order NLO responses have been determined (assumed to be real because the imaginary part has been neglected) from the experimental value γ_{EFISH}, through eq 1:

$$\gamma_{EFISH} = \frac{\mu\beta_\lambda(-2\omega;\omega,\omega)}{5kT} + \gamma(-2\omega;\omega,\omega,0) \qquad (1)$$

where γ_{EFISH} is the sum of a cubic electronic contribution $\gamma(-2\omega;\ \omega,\ \omega,\ 0)$ and of a quadratic dipolar contribution $\mu\beta_\lambda(-2\omega;\omega,\omega)/5kT$, with μ being the ground state dipole moment and β_λ the projection along the dipole moment axis of the vectorial component β_{vec} of the tensorial quadratic hyperpolarizability working with an incident wavelength λ.

$\beta_\lambda(-2\omega;\omega,\omega)$ has been determined from the experimental value of γ_{EFISH} using the DFT calculated value of the dipole moment μ and neglecting the cubic electronic contribution $\gamma(-2\omega;\omega,\omega,0)$, since the porphyrinic NLO chromophores **1** and **3** are characterized by a large dipole moment[3,7,9] and therefore by a high dipolar contribution to γ_{EFISH}.[15]

PGSE NMR Measurements. ^{1}H PGSE (pulsed field gradient spin−echo) NMR measurements have been performed at 295.7 K without spinning by using the standard stimulated echo pulse sequence[16] on a Bruker AVANCE DRX 400 spectrometer equipped with a GREAT 1/10 gradient unit and a QNP probe with a Z-gradient coil. The shape of the gradients was rectangular, their duration (δ) was 4 ms, and their strength (G) has been varied during the experiments. All spectra have been obtained using 32K points and a spectral width of 5000 Hz, and they have been processed with a line broadening of 1.0 Hz. Different values of "nt" (number of transients) and number of different gradient strengths (G) have been used for different samples, depending on solution viscosity and solute concentration. The dependence of the resonance intensity (I) on a constant

diffusion time and on a varied gradient strength (G) is given by eq 2:

$$\ln \frac{I}{I_0} = -(\gamma\delta)^2 D_t\left(\Delta - \frac{\delta}{3}\right)G^2 \quad (2)$$

where I is the intensity of the observed spin echo, I_0 is the intensity of the spin echo without gradients, D_t is the diffusion coefficient, Δ is the delay between the midpoints of the gradients, δ is the length of the gradient pulse, and γ is the magnetogyric ratio. The semilogarithmic plots of $\ln(I/I_0)$ vs G^2 have been fitted using the standard linear regression algorithm implemented in the Origin 7 software package, and the R factor was always higher than 0.99. For pure solvents, the diffusion coefficient D_t, which can be evaluated from the slope of the regression line obtained by plotting $\ln(I/I_0)$ vs G^2, has been estimated by taking as reference a sample of HDO (0.04%) in D_2O (known diffusion coefficient in the range 274−318 K)[17] under the exact same experimental conditions as those for the sample of the porphyrin. TMSS (tetrakis-(trimethylsilyl)silane) has been used as internal standard to account for possible changes in solution viscosity, temperature, and gradient strength.[18] The experimental error on D_t has been estimated to be 3% for all the solutions investigated except those with concentration smaller than 10^{-5} M. In this latter case, the error can approach 5−8%.

Theoretical Calculations. All the calculations have been performed by the Gaussian03 program package.[19] For DFT, the B3LYP functional,[20] and 6-311 g*/6-31g* have been used for the Zn, O, N, C, and H atoms, respectively.[21] The geometries have been optimized by DFT, and dipole moments have been calculated according to the optimized geometries; for the monomers (dimers), a C_{2v} (C_s) symmetry has been considered. Hyperpolarizabilities have been computed by coupled-perturbed-HF (both static and frequency-dependent) and coupled-perturbed DFT/finite-field (static) procedures. Solvation effects ($CHCl_3$) on the absorption spectra and hyperpolarizabilities have been investigated by PCM/C-PCM approaches.[22−24] We previously found that for **1** the absorption spectra and NLO properties *in vacuo* provide a better match with experimental quantities.[9] We therefore mainly refer to results obtained *in vacuo*, if not otherwise indicated. Absorption spectra have been simulated by a Gaussian convolution with $\sigma = 0.20$ eV, corresponding to a fwhm of ca. 0.48 eV. Based on the selected fwhm, molar extinction coefficients were also calculated. Hyperpolarizabilities are reported according to the phenomenological convention.[25]

Synthesis of [5-[(4′-(Dimethylamino)phenyl)ethynyl]-15-[(4″-nitrophenyl)ethynyl]-10,20-diphenylporphyrinate]-Zn(II) (1). The synthesis has been performed by a two step process. For the attribution of the ^{1}H NMR signals, see the following:

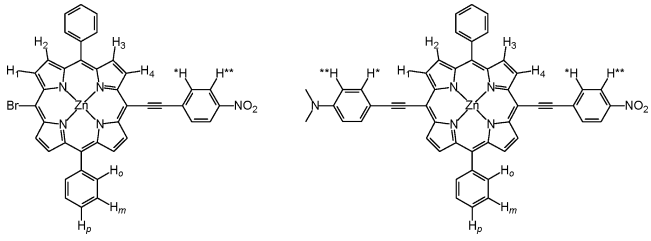

First Step: Synthesis of [5-[(4-Nitrophenyl)ethynyl]-15-bromo-10,20-diphenylporphyrinate]Zn(II). [5-Iodo-15-bromo-10,20-diphenylporphyrinate]Zn(II)[13] (100 mg, 0.137 mmol), CuI (13.5 mg, 0.068 mmol), $[Pd(PPh_3)_2Cl_2]$ (6 mg, 0.008 mmol), and NEt_3 (1.37 mmol, 0.2 mL) were introduced in a Schlenk tube under nitrogen atmosphere. The mixture was then degassed three times with a vacuum−nitrogen cycle, ending on nitrogen, before addition of dry THF (50 mL) and of 4-nitrophenylacetylene (22.8 mg, 0.151 mmol). The solution was left at room temperature for 24 h. After elimination under high vacuum of the solvent, the crude product, supported on Florisil, was purified by column chromatography on silica gel, by elution with n-hexane/THF = 8/2, affording 70 mg (68%) of the compound.

^{1}H NMR (300 MHz, $CDCl_3$ with addition of excess pyridine-d_5 in order to obtain an acceptable solubility): 9.64 (d, 2H, H_1, J = 4.7 Hz), 9.63 (d, 2H, H_4, J = 4.7 Hz), 8.89 (d, 2H, H_2, J = 4.7 Hz), 8.82 (d, 2H, H_3, J = 4.7 Hz), 8.34 (d, 2H, $H^{**}_{NO_2}$, J = 8.8 Hz), 8.16 (m, 4H, Ho), 8.02 (d, 2H, $H^{*}_{NO_2}$, J = 8.8 Hz), 7.77 (m, 6H, Hm, Hp). Anal. Calcd for $C_{40}H_{22}BrN_5O_2Zn$: C, 64.06; H, 2.96; N, 9.34. Found: C, 64.69; H, 3.12; N, 8.98.

Second Step: Synthesis of [5-[(4′-Dimethylamino)phenyl]-ethynyl]-15-[(4″-nitrophenyl)ethynyl]-10,20-diphenylporphyrinate]Zn(II) (1). [5-[(4-Nitrophenyl)ethynyl]-15-bromo-10,20-diphenylporphinato]Zn(II) (50.0 mg, 0.667 mmol), $[Pd(PPh_3)_2Cl_2]$ (2.3 mg, 0.0026 mmol), CuI (1.3 mg, 0.0064 mmol), and NEt_3 (1.362 mmol, 0.2 mL) were introduced in a Schlenk tube under nitrogen atmosphere. Fifteen milliliters of CH_3CN and 10 mL of dry THF were added, and the mixture was degassed five times at −78 °C with a vacuum−hydrogen cycle, ending on hydrogen. In another Schlenk tube, a solution of 4-dimethylaminophenylacetylene (11.3 mg, 0.075 mmol) in 5 mL of CH_3CN was degassed in a similar way and subsequently added to the refluxing reaction mixture. The resulting solution was refluxed for 24 h. After elimination under high vacuum of the solvent, the crude product, supported on Florisil, was purified by column chromatography on silica gel, by elution with n-hexane/THF = 8/2, affording 9 mg (16.6%) of **1**.

^{1}H NMR (400 MHz, $CDCl_3$ with addition of excess pyridine-d_5): 9.71 (d, 2H, H_1, J = 4.5 Hz,), 9.62 (d, 2H, H_4, J = 4.6 Hz), 8.86 (d, 2H, H_2, J = 4.6 Hz), 8.80 (d, 2H, H_3, J = 4.5 Hz), 8.39 (d, 2H, $H^{**}_{NO_2}$, J = 8.9 Hz), 8.20 (m, 4H, Ho), 8.09 (d, 2H, $H^{*}_{NO_2}$, J = 8.9 Hz), 7.88 (d, 2H, $H^{*}_{NMe_2}$, J = 8.9 Hz), 7.76 (m, 6H, Hm, Hp), 6.86 (d, 2H, $H^{**}_{NMe_2}$, J = 8.9 Hz), 3.08 (s, 6H, NMe_2). Anal. Calcd for $C_{50}H_{32}N_6O_2Zn$: C, 73.76; H, 3.96; N, 10.32. Found: C, 73.89; H, 3.87; N, 10.41.

3. Results and Discussion

3.1. Synthesis of the NLO Chromophores. The Zn(II) porphyrinate **1** has been prepared with a modification of the method reported in the literature[3] (see Experimental Section) that we were unable to reproduce with acceptable yields, despite several attempts. Our experimental approach, reported in Scheme 1, takes advantage of the structural asymmetry of the intermediate [5-iodo-15-bromo-10,20-diphenylporphyrinate]Zn(II)[13] instead of the intermediate [5,15-dibromo-10,20-diphenylporphyrinate]Zn(II),[3] in which the different reactivity of the carbon−iodine and carbon−bromine bonds allows a more facile two step process of coupling the two different acetylenic moieties to the positions 5 and 15 of the porphyrin ring.

Therefore, by Sonogashira coupling we introduced first the electron acceptor 4-nitrophenylacetylene moiety and then the electron donor 4-dimethylaminophenylacetylene moiety. In the second step, in order to drastically reduce the undesired side homocoupling reaction of 4-dimethylaminophenylacetylene, the reaction was carried out under hydrogen atmosphere.[26] The Ni(II) porphyrinate **3** has been synthesized according to the literature.[7]

SCHEME 1: Synthesis of the Zn(II) NLO Chromophore 1

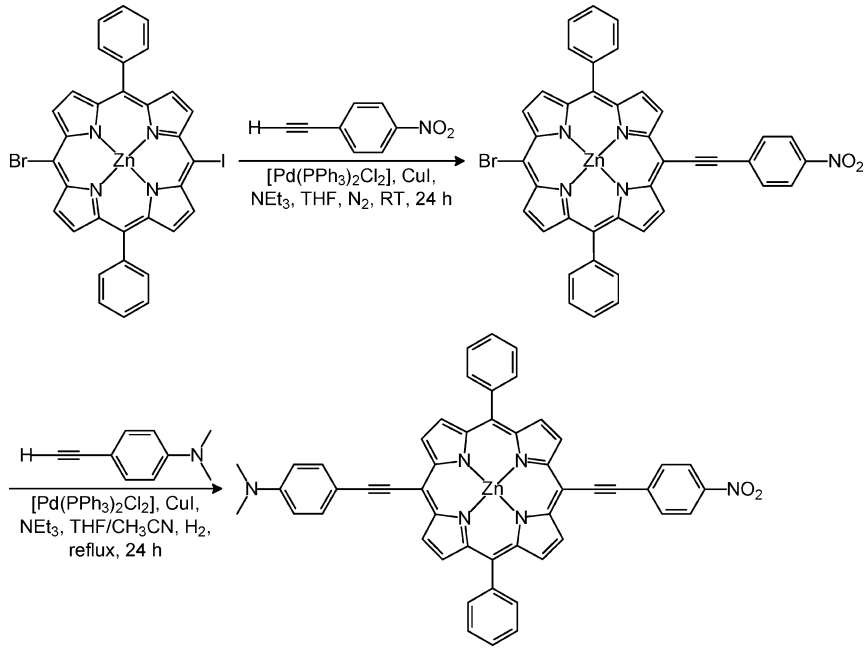

TABLE 1: Electronic Absorption Spectral Data (λ_{max}) of the B and Q Bands and EFISH $\mu\beta_{1.907}$ as a Function of the Concentration and of the Solvent for the Zn(II) NLO Chromophore 1

conc (mol L^{-1})	solvent	λ_{max} (log ε) (nm)	$\mu\beta_{1.907}$ ($\times 10^{-48}$ esu)	$\beta_{1.907}$ ($\times 10^{-30}$ esu)
5×10^{-5}	$CHCl_3$	452[a] (4.82)	6093	438[c]
		669[b] (4.36)		
10^{-5}	$CHCl_3$	452[a] (4.81)	5438	391[c]
		667[b] (4.35)		
5×10^{-6}	$CHCl_3$	452[a] (4.89)	6412	461[c]
		663[b] (4.43)		
10^{-6}	$CHCl_3$	452[a] (4.99)	nd	nd
		663[b] (4.50)		
5×10^{-5}	$CHCl_3$ + pyridine	464[a] (5.15)	2921	208[d]
		689[b] (4.74)		
5×10^{-5}	DMF	460[a] (5.04)	2600	188[c]
		685[b] (4.66)		

[a] λ_{max} of the B band. [b] λ_{max} of the major Q-band. [c] $\mu = 13.9$ D calculated by DFT (see ref 9). [d] $\mu = 14.0$ D calculated by DFT for the adduct with pyridine in the axial position (**1-py**).

TABLE 2: Electronic absorption spectral data (λ_{max}) of B and Q bands and EFISH $\mu\beta_{1.907}$ as a function of the concentration and of the solvent for Ni(II) NLO chromophore 3

conc (mol L^{-1})	solvent	λ_{max} (log ε) (nm)	$\mu\beta_{1.907}$ ($\times 10^{-48}$esu)	$\beta_{1.907}$[d] ($\times 10^{-30}$ esu)
7.5×10^{-4}	$CHCl_3$	459[a] (sat.)[b]	676	50
		633[c] (4.60)		
2×10^{-4}	$CHCl_3$	459[a] (5.04)	1200	90
		633[c] (4.63)		
5×10^{-5}	$CHCl_3$	458[a] (5.05)	3076	230
		632[c] (4.63)		
10^{-5}	$CHCl_3$	451[a] (4.98)	nd	nd
		627[c] (4.45)		
10^{-6}	$CHCl_3$	451[a] (4.85)	nd	nd
		625[c] (4.37)		
5×10^{-5}	$CHCl_3$ + pyridine	458[a] (5.04)	2627	196
		632[c] (4.62)		
5×10^{-5}	DMF	452[a] (4.85)	2864	214
		637[c] (4.53)		

[a] λ_{max} of the B band. [b] "sat." means "under saturation conditions". [c] λ_{max} of the major Q-band. [d] $\mu = 13.4$ D calculated by DFT.[9]

3.2. Experimental EFISH Investigation of the Second Order NLO Properties of 1 and 3. The investigation of the second order properties of the NLO chromophores **1** and **3** has been carried out by the EFISH technique,[8] working with a nonresonant incident wavelength of 1.907 μm, and in solvents of different dielectric constant and donor properties such as $CHCl_3$ and DMF in order to explore the role of the polarity and donor properties of the solvent in tuning the second order NLO response. Solutions of **1** and **3** in $CHCl_3$ after addition of 0.1−0.2% volumes of pyridine have also been investigated in order to avoid possible aggregations, which may take place, particularly in $CHCl_3$ solution. Measurements in $CHCl_3$ have been carried out in a range of concentrations between 5×10^{-5} M and 5×10^{-6} M in the case of the less soluble **1** (Table 1) and in the range between 7.5×10^{-4} M and 5×10^{-5} M in the case of the more soluble **3** (Table 2). In DMF or in $CHCl_3$ added with excess pyridine, only the 5×10^{-5} M concentration has been investigated for both **1** and **3**.

The values of the ground state dipole moments of **1** and **3** have been recently calculated at the DFT level of theory (13.9 and 13.4 D *in vacuo* and 16.0 and 15.2 D in $CHCl_3$ solution, respectively).[9] In this work a value of 14.0 D for the dipole moment of the adduct of **1** with pyridine (**1-py**) has been calculated *in vacuo* at the DFT level of theory (see section 3.4). It must be pointed out that for **1-py**, DFT calculations have evidenced a 4.5 D dipole component perpendicular to the porphyrin plane, thus producing a slightly deviated orientation of the axis of the dipole moment of **1-py** when compared to that of **1** and **3**, which is along the push−pull system.[9] These theoretical dipole moment values have been used to evaluate the quadratic hyperpolarizabilities of **1** and **3** from EFISH measurements according to eq 1 (Tables 1 and 2).

For the NLO chromophore **1**, the $\beta_{1.907}$ values in $CHCl_3$ solution remain rather constant in the range of concentration investigated (within the experimental error of ±15%), with the mean value being about 430×10^{-30} esu (Table 1). In a solvent of higher dielectric constant and with some donor properties, such as DMF or $CHCl_3$ after addition of pyridine, the $\beta_{1.907}$ values, all measured at the same concentration (5×10^{-5} M),

are not only similar (188×10^{-30} esu and 208×10^{-30} esu, respectively) but about half of the value of **1** measured at the same concentration in $CHCl_3$ solution (438×10^{-30} esu). These striking differences are due to the axial coordination of a donor ligand such as pyridine or to the donor properties, together with the increased dielectric constant, of DMF, which both prevent aggregation processes. Therefore, these lower $\beta_{1.907}$ values should represent the value of the quadratic hyperpolarizability of a monomeric species of **1**, such as the adduct **1-py** or the species solvated by DMF. In $CHCl_3$ solution some aggregation could take place, producing a significant increase of the value of the quadratic hyperpolarizability (Table 1).

Unlike the Zn(II) NLO chromophore **1**, the $\beta_{1.907}$ value of the Ni(II) NLO chromophore **3** in $CHCl_3$ solution increases with decreasing concentration (Table 2), reaching, at 5×10^{-5} M concentration, a value of 230×10^{-30} esu, corresponding to almost half of the value measured in $CHCl_3$ for **1** at the same concentration (438×10^{-30} esu; see Table 1). Therefore, in $CHCl_3$ solution the metal (Zn(II) in **1** and Ni(II) in **3**) may play a relevant role in controlling the value of the quadratic hyperpolarizability, as previously suggested, while working in DMF or in $CHCl_3$ added with 0.1−0.2% volumes of pyridine, the value of $\beta_{1.907}$ for both **3** and **1**, at 5×10^{-5} M concentration, is comparable (214×10^{-30} esu and 196×10^{-30} esu against 188×10^{-30} esu and 208×10^{-30} esu, respectively) and also comparable to the value of **3** measured in $CHCl_3$ solution at the same concentration (230×10^{-30} esu) (Tables 1 and 2). It follows thus that **3**, at 5×10^{-5} M concentration, is probably present mainly as a monomeric species even in $CHCl_3$ solution. The significant decrease in $CHCl_3$ solution of the $\beta_{1.907}$ value of **3** up to about $50-90 \times 10^{-30}$ esu by increasing concentration (Table 2) would suggest an aggregation process, but completely different from that occurring to **1** in $CHCl_3$ solution.

In summary, EFISH measurements give evidence that, when working in the absence of aggregation processes (as in DMF solution or in $CHCl_3$ solution with addition of excess pyridine), the $\beta_{1.907}$ values for both **1** and **3** are similar and consequently not affected by the nature of the metal, in agreement with the results of the CP-DFT and CP-HF theoretical calculations.[9]

Moreover, the EFISH $\beta_{1.907}$ value of **1**, measured in $CHCl_3$ solution, is always lower than the $\beta_{1.06}$ value measured, still in $CHCl_3$ solution, by the HRS technique[3] or obtained by the method based on the Stark effect.[5] It must be noticed that the use of an incident wavelength of 1.064 μm may produce a large increase of the value of the quadratic hyperpolarizability due to dispersion effects, which introduces a resonance enhancement of the second harmonic, as also suggested by CP-HF theorethical calculations.[9]

In any case, such striking differences cannot be attributed to the different experimental techniques (HRS for **1**[3] and EFISH for **3**[7]), since HRS β_{zzz}, the only significant tensor component for this kind of push−pull NLO chromophores, does correspond to EFISH β.[9]

As just noticed, the different trends with concentration of the second order NLO response of **1** and **3** in $CHCl_3$ solution (Tables 1 and Tables 2) would suggest different processes of aggregation. For the less soluble Zn(II) NLO chromophore **1**, the larger $\beta_{1.907}$ values, even in diluted solutions, would suggest the presence of a certain amount of head to head fashion aggregation (J-aggregate), which should produce an increase of the second order NLO response.[27] On the other hand, for the more soluble NLO chromophore **3**, a process of head-to-tail fashion aggregation (H aggregate) seems to occur at least at higher concentrations, as reflected by the progressive decrease of the EFISH $\beta_{1.907}$ value with increasing concentration (Table 2).

3.2. Electronic Absorption Spectra. Electronic absorption spectra of chromophores **1** and **3** have been recorded in $CHCl_3$ solution, in the concentration ranges 5×10^{-5} M to 10^{-6} M for **1** and 7.5×10^{-4} M to 10^{-6} M for **3.** In DMF solution and in $CHCl_3$ solution with addition of 0.1−0.2% volumes of pyridine, the spectra do not change with concentration; therefore, for these two solvents, only the absorption data at 5×10^{-5} M concentration are reported (Tables 1 and 2). In all the solvents, **1** and **3** show the expected two major electronic absorption bands: the very strong B band, between 450 and 460 nm, and a quite strong Q-band, between 660 and 685 nm for **1** and 625 and 635 nm for **3**.

While in DMF or in $CHCl_3$, with addition of pyridine, the spectrum of **1** follows the Lambert−Beer law, in $CHCl_3$ slight deviations from the Lambert−Beer law have been observed at higher concentrations for the Q-band. In accordance, while the wavelength of the maximum of the B band does not change with concentration, that of the Q-band shows a very small red shift of 5−6 nm with increasing concentration.

The spectrum of **1** shows a red shift of the wavelengths of both the B and Q bands (Table 1) in DMF or in $CHCl_3$ with addition of pyridine, as expected for an axial interaction of DMF and pyridine with the Zn(II) center.[28]

The spectra of **3** in $CHCl_3$ and in DMF solution or in $CHCl_3$ solution with addition of 0.1−0.2% volumes of pyridine (Table 2) are comparable, thus confirming the absence of an axial interaction of the NI(II) center of **3** with both DMF and pyridine, as suggested by the EFISH investigation.

In a $CHCl_3$ solution of **3**, a shift of the wavelength of the maximum of the Q-band (from 633 to 625 nm), with a slight decrease of the intensity (log ε from about 4.6 to about 4.4) and of the B band (from 459 to 451 nm), occurs by dilution up to 10^{-6} M.

It follows that the presence of some aggregation (H or J) in $CHCl_3$ solution suggested by the EFISH investigation does not seem to be clearly supported by electronic absorption spectra, which are very little influenced by changing the concentration.

3.4. Theoretical Calculations. ***3.4.1. Pyridine Adduct of 1 and 3.*** A theoretical DFT/TDDFT investigation and coupled perturbed CP-DFT/CP-HF calculations *in vacuo* have been carried out in order to define the optimized geometry and the value of the dipole moment and to reproduce both the electronic absorption spectrum and the value of the quadratic hyperpolarizability of the adduct of **1** and **3** with pyridine. Similar theoretical calculations have been previously carried out by some of us for the chromophores **1** and **3**.[9]

The DFT optimized geometrical structures for the adducts of **1** with one and two pyridines are reported in Figure 2. The calculated interaction energy between **1** and one pyridine provides a value of 11.1 kcal/mol, confirming the experimental evidence for a quite stable pentacoordinated adduct (**1-py**), while the adduct with two pyridines has been found to be only 2.5 kcal/mol more stable than the adduct with one pyridine and, consequently, little probable. The adduct of **3** with one pyridine has been found to be only 0.8 kcal/mol more stable than the free reagents, thus confirming that the formation of such an adduct is quite unlikely, as suggested by electronic absorption spectra and EFISH investigation.

TDDFT calculated absorption spectra of **1** and its pyridine adduct (**1-py**) have evidenced the expected red shift of both B and Q bands for **1-py** when compared to **1** (Figure 3).

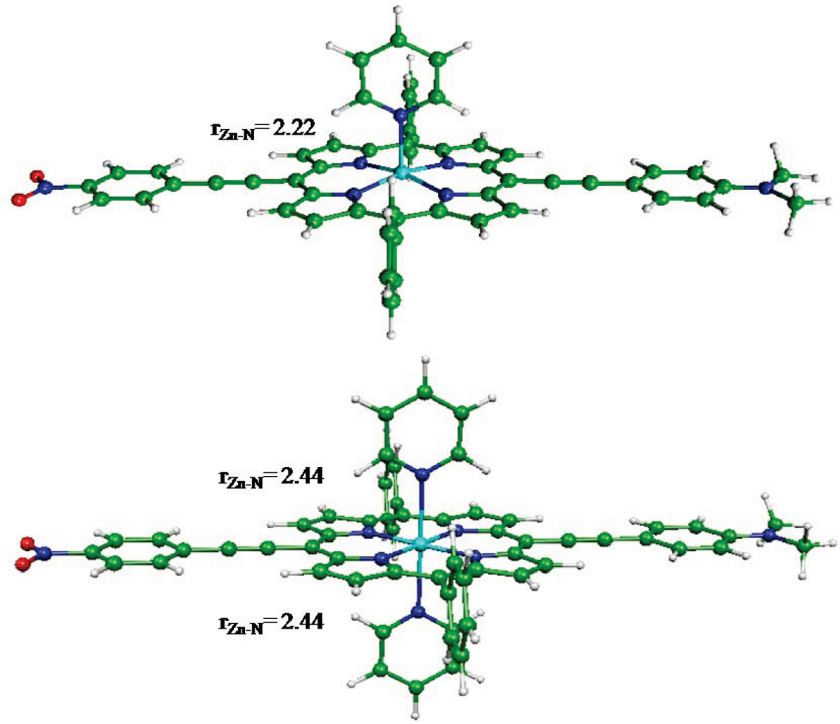

Figure 2. Optimized molecular structure of **1-py** and **1** with two pyridine molecules.

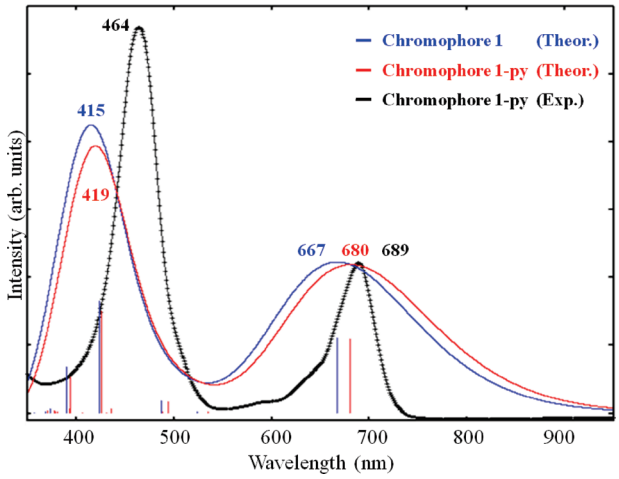

Figure 3. Comparison between the calculated absorption spectra of the chromophores **1** and **1-py** and the experimental spectrum of **1-py**.

Comparison of the calculated spectrum of **1-py** with the experimental spectrum recorded in $CHCl_3$ after addition to **1** of excess pyridine has evidenced a very good agreement of the λ_{max} of the major Q-band (680 vs 689 nm, respectively). The calculated molar extinction coefficients for this band are overestimated by about 20% compared to experimental values ($\varepsilon \approx 60000$ vs 50000). Nevertheless, the relative intensities of the absorption maxima of the Q and B bands are accurately reproduced; see Tables 1 and 3. The Q-band represents in both **1** and **1-py** the HOMO−LUMO charge transfer transition from the donor to the acceptor part of the push−pull system of this kind of NLO chromophores, which controls the value of the quadratic hyperpolarizability.[9] Such good agreement, as expected, was not found when comparing the calculated absorption spectrum of **1** (which represents a monomeric species) and its experimental spectrum in $CHCl_3$[9] (which represents an aggregate species).

The calculated CP-HF and CP-DFT values of the static hyperpolarizability, β_0, and the CP-HF values of the frequency dependent hyperpolarizability, $\beta_{1.907}$, the hyperpolarizability for both **1** and **1-py** (Table 3) are in accordance with the conclusions reached by the EFISH investigation. The DFT β_0 value for **1-py** (333×10^{-30} esu) is comparable with the corresponding value of **1** (301×10^{-30} esu)[9] and in acceptable agreement with the experimental EFISH value of **1** measured working at 1.907 μm incident wavelength in DMF or in $CHCl_3$ solution after addition of excess pyridine (188 and 208 $\times 10^{-30}$ esu, respectively).

3.4.2. J and H aggregates of 1 and 3. The possible process of aggregation in a $CHCl_3$ solution of **1** has been investigated by DFT/TDDFT CP-HF calculations. Two dimeric arrangements have been taken into consideration: one corresponding to a J aggregation (head-to-head) and one corresponding to a H aggregation (head-to-tail). The structures of these two aggregates optimized by DFT are reported in Figure 4.

It can be noticed that the dimeric aggregation induces in both cases a substantial geometrical deformation of the two interacting porphyrinic chromophores. This deformation is dictated by a weak donor−acceptor bonding interaction which takes place between the NMe_2 donor group of one porphyrinate and the Zn(II) acceptor center of the other porphyrinate, as evidenced by Zn−NMe_2 calculated distances of 2.67 and 2.70 Å. Such kind of dimeric aggregation dictated by donor−acceptor interactions between two porphyrinic units was reported for instance in $CHCl_3$ solution for the complementary coordination of the imidazolyl substituent of one imidazolyl porphyrinate Zn(II) unit to the Zn center of another imidazolyl porphyrinate Zn(II) unit.[29] In the case of the J aggregation of **1**, a very weak interaction occurs between the Zn(II) center of one porphyrinate and the NO_2 group of the other porphyrinate unit, with Zn−O and Zn−N distances of 3.30 and 3.38 Å, respectively.

The H and J dimeric aggregates of **1** are almost isoenergetic, with the H dimer being more stable than the J dimer by only 2.2 kcal/mol. This small energy difference would suggest that both species are equally probable, within the accuracy of

TABLE 3: Dipole Moments (μ, D), β^0_{zzz} and β^{λ}_{zzz} (10^{-30} esu) ($\lambda = 1.907$ μm), and λ_{max} (nm) for the Q and B Bands (log ε Values in Parentheses) of 1 and 1-py and of the H and J Dimers Calculated at the HF and DFT Levels of Theory

	1				1-py				J-dimer of 1				H-dimer of 1			
	μ(D)	β^0_{zzz}	β^{λ}_{zzz}	λ_{max} (nm)	μ (D)	β^0_{zzz}	β^{λ}_{zzz}	λ_{max} (nm)	μ (D)	β^0_{zzz}	β^{λ}_{zzz}	λ_{max} (nm)	μ (D)	β^0_{zzz}	β^{λ}_{zzz}	λ_{max} (nm)
HF	12.7	66	76	362 (4.13) 697 (5.33)	12.9	65	70		21.4	111	116		0.0	0.0	0.0	
DFT	13.9	301	n.d.	415 (5.09) 667 (4.80)	14.0	333	n.d.	419(5.06) 680(4.80)	23.1	606	n.d.	421(5.38) 672(5.09)	0.0	0.0	n.d.	425(5.36) 664(5.09)

calculations. The calculated energies of the H and J dimers are at 7.5 and 5.3 kcal/mol below the energy of two noninteracting porphyrinic units, in good agreement with the experimental Gibbs free energy of dimerization obtained for **1** by PGSE NMR measurements, which has provided values of the order of 5−6 kcal/mol (see section 3.5). Most notably, no stable dimeric species could be computed for the NLO chromophore **3**. In the latter case, every attempt to optimize the geometry of dimeric H or J aggregates has provided an increase of energy of about 10 kcal/mol.

A schematic representation of the frontier molecular orbitals of **1** and of its J dimer calculated at the DFT level of theory is reported in Figure 5, along with isodensity plots of the HOMO − 1/HOMO/LUMO/LUMO + 1 for the J dimer.

The formation of the J dimer introduces some sizable perturbation of the electronic structure. In particular, taking two isolated porphyrinic units as reference, the two couples of initially degenerate HOMO and LUMO orbitals split upon dimerization to a J aggregate as a consequence of the excitonic interactions.[27] The calculated HOMO splitting is smaller than

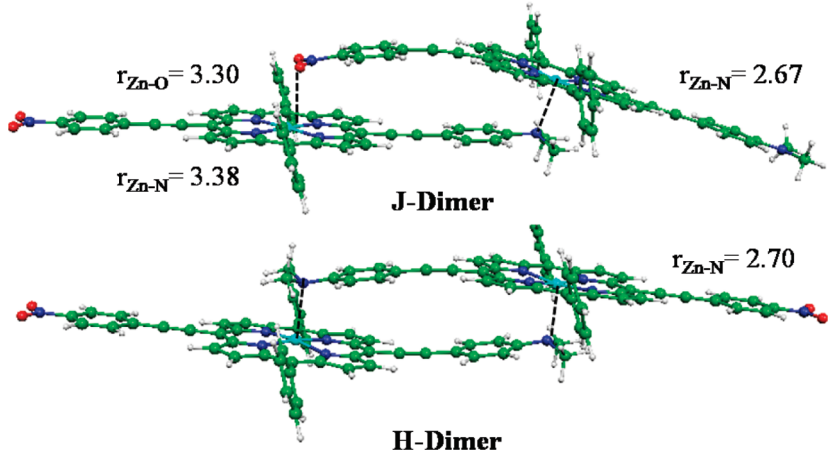

Figure 4. Optimized structures of J and H dimeric aggregates of the NLO chromophore **1**, together with the main optimized geometrical parameters (Å).

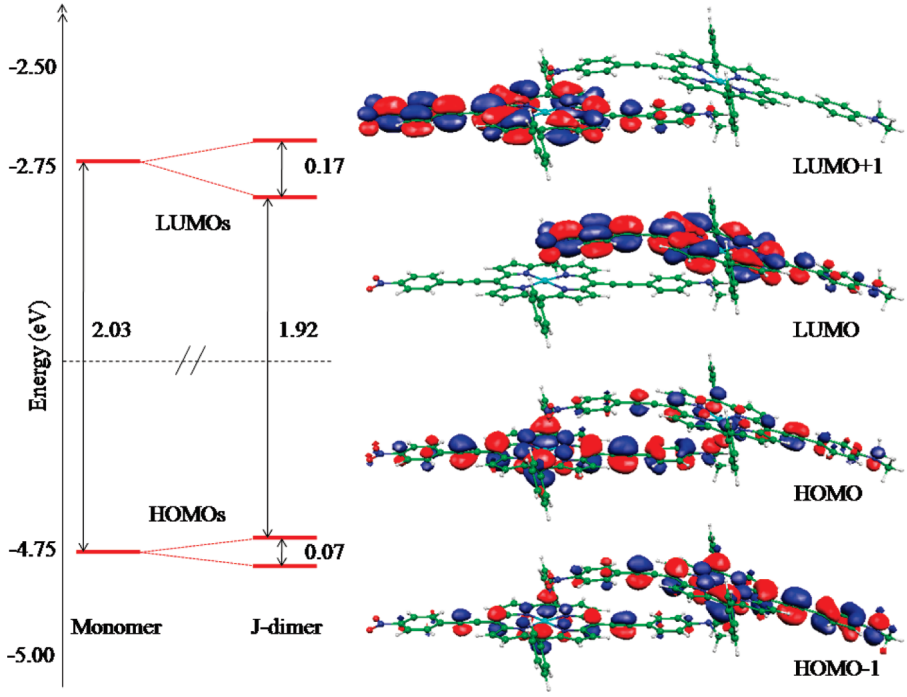

Figure 5. Comparison between the HOMOs−LUMOs calculated molecular orbitals of **1** and those of the corresponding J dimeric aggregate and isodensity plots of selected molecular orbitals of the J dimeric aggregate.

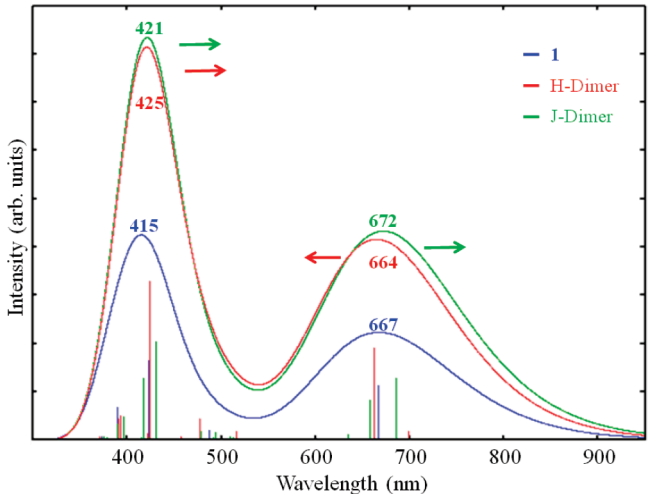

Figure 6. Comparison between the calculated absorption spectra of **1** and those of its H and J dimeric aggregates. The intensity of the dimer is nearly twice that of **1**, since it has two chromophoric units.

the LUMO one (0.07 and 0.17 eV, respectively). While the HOMOs are partly delocalized across the two interacting chromophores, the LUMOs turn out to be almost entirely localized on either one of the two interacting chromophores. As a consequence, the J dimer shows a slightly reduced HOMO−LUMO gap compared to that of the single porphyrinic chromophore **1** (1.92 vs 2.03 eV, respectively).

Calculated electronic absorption spectra for **1** and both the H and J dimers of **1** are reported in Figure 6.

The calculated absorption spectra of J and H dimers of **1** are, apart from the expected almost doubled intensity, similar to that of **1**, as experimentally observed. Small differences are however to be noticed: for the H dimer, a slight blue (red) shift of the Q (B) band is calculated, while, for the J dimer, both B and Q bands are slightly red-shifted (Table 3). Overall, it seems that, despite the rather large geometrical distortion accompanying the formation of both dimers, its impact on the electronic absorption spectra is very limited.

A comparison between the experimental absorption spectrum in $CHCl_3$ of **1** at 5×10^{-5} M concentration (Table 1) and that calculated at the DFT level of theory for a dimeric J aggregate of **1** (which from EFISH measurements seems to be the aggregate species present in $CHCl_3$ solution at 5×10^{-5} M concentration) shows an excellent agreement of the λ_{max} of the Q-band (669 nm vs 672 nm where 672 is the main value of three calculated transitions) while the calculated λ_{max} of the B band (421 nm) is slightly underestimated compared to the experimental value of 452 nm (Table 3); the 0.2 eV deviation between computed and experimental values is of the same order as the accuracy of the employed methodology.

Inspection of the TDDFT eigenvectors allows us to gain a major insight into the nature of the transitions most contributing to the electronic absorption spectrum of the J dimer of **1**. The quite strong Q-band has been reported to be constituted by a single and intense transition, involving excitation from the HOMO to the LUMO, calculated at 1.86 eV (667 nm), with an oscillator strength f of 1.12.[9] For the dimeric J aggregate of **1**, the expected red-shifted excitation involving the HOMOs and the LUMOs is calculated at 1.55 eV (801 nm) but of negligible intensity ($f = 0.01$). Such very low intensity explains why we could not detect the red-shifted new absorption band, expected for J aggregation, in the experimental absorption spectrum of **1** in $CHCl_3$ solution. The Q-band appears to be mainly composed of three excitations, a major one calculated at 1.81 (685 nm), and two minor ones at 1.89 (658 nm) and 1.95 eV (635 nm), with oscillator strengths f of 1.28, 0.82, and 0.11, respectively. These transitions involve the HOMO − 1 → LUMO, HOMO → LUMO + 1, and HOMO − 1→ LUMO + 1 excitations, respectively. The total calculated oscillator strength of the Q-band of the J dimer of **1** is almost twice that calculated for **1**, indicating that the interaction of the two porphyrinic chromophores does not produce any substantial increase of the intensity of the Q-band. The calculated excited state dipole moment of the intense 685 nm HOMO − 1 → LUMO transition of the J dimer provides a total value of 42.5 D, essentially aligned along the main symmetry axis, while the calculated ground state total dipole is 23.1 D. The dipole moment variation $\Delta\mu_{eg}$ accompanying this transition is therefore 19.4 D, comparable to the 21.7 D value calculated in the case of **1** for its HOMO − LUMO transition corresponding to the Q-band.[9]

In conclusion, our calculations have shown that aggregation of **1** to form a dimeric J aggregate does not produce relevant changes of the λ_{max} and intensity of the Q-band and that the intensity of the new absorption band at lower energy typical of J aggregation is too low to be detected in the experimental electronic absorption spectrum.

For the J dimeric aggregate of **1**, we have thus calculated both the static β_0 and frequency dependent $\beta_{1.907}$ quadratic hyperpolarizabilities by means of CP-HF calculations, since by CP-DFT we could compute only β_0 by means of finite-field differentiation of analytic polarizabilities. The calculated values, including the dominant dipole moment components, have been compared with those obtained for **1**[9] and **1-py** still by CP-HF calculations (Table 3).

By comparing the dipole moment and the value of the quadratic hyperpolarizability, $\beta_{1.907}$, of the J dimeric aggregate of **1** with those of **1** considered as a monomer, the dimerization is accompanied by an almost doubling of both parameters, in agreement with the main conclusions reached by previous ZINDO/CV theoretical calculations.[27] For the J dimeric aggregate of **1**, a small dipole component orthogonal to the main axis of the dimer has been calculated (2.6 and 3.0 D at the HF and DFT levels of theory, respectively), while for **1** the only nonzero dipole moment component is aligned along the main symmetry axis of the push−pull system.[9] For the J dimeric aggregate the main component of the quadratic hyperpolarizability is directed along the dipole moment molecular axis (β_{zzz} tensor), with all the other components being at least 1 order of magnitude smaller, as it was reported to occur in the case of **1**. Static quadratic hyperpolarizability β_0 values of 111×10^{-30} esu and of 606×10^{-30} esu are calculated at the HF and DFT levels of theory, respectively, to be compared to β_0 values of 66×10^{-30} esu and 301×10^{-30} esu calculated for **1**.[9] Although the calculated β_0 values at the CP-HF and CP-DFT levels of theory are, as already observed,[9] quite different, the trend is similar. Therefore, at any level of theory, the perturbation introduced by J aggregation on the second order NLO response of **1** produces an increase of about two times the value of the quadratic hyperpolarizability. This conclusion not only confirms the results of the EFISH investigation, which has shown a similar increase in $CHCl_3$ solution, when compared to the value measured in DMF solution (Table 1), but it also supports, as already suggested by the EFISH investigation, that in $CHCl_3$ solution the chromophore **1** dimerizes, at least in part, as a J aggregate.

3.5. PGSE NMR Study. PGSE NMR experiments have been carried out in order to estimate the level and nature of

TABLE 4: Diffusion Coefficients ($10^{10}D_t$ m^2 s^{-1}), *P* Factor (Å), Dimerization Equilibrium Constant (K_D, M^{-1}) and Mole Fractions of the Dimer (x_D) for 1 and 3 as a Function of the Solvent and of the Molar Concentration *C* (M)

					model 1		model 2		
entry	compd	solvent	D_t	P	K_D	x_D	K_D	x_D	C
1	**1**	$CDCl_3$	5.46	42.27	1.75×10^5	0.60	9×10^3	0.16	3×10^{-5}[a]
2	**1**	$CDCl_3$ + 0.4%THF	5.31	41.63	1×10^5	0.50	9.3×10^3	0.17	3×10^{-5}[a]
3	**1-py**[b]	$CDCl_3$	5.71	39.97					2.1×10^{-4}
4	**1**	$C_6D_5NO_2$	1.60	40.13	1×10^5	0.30	1.5×10^4	0.08	6×10^{-6}
5	**1**	$C_6D_5NO_2$	1.56	42.11	1.5×10^5	0.60	5×10^3	0.17	6×10^{-5}[a]
6	**3**	$CDCl_3$	5.78	38.28		0		0	7×10^{-5}
7	**3** + py[c]	$CDCl_3$	5.84	38.40		0		0	3.8×10^{-4}
8	**3**	$CDCl_3$	5.82	39.99	1×10^3	0.20	1.5×10^2	0.06	4.7×10^{-4}

[a] Saturated solution. [b] py = pyridine, 0.065 M. [c] py = pyridine, 0.050 M.

aggregation of **1** and **3** in $CHCl_3$ solution. Due to the rather poor solubility, in particular of **1** but also of **3** in $CHCl_3$, PGSE measurements have required very long acquisition time (up to days) and the limit of sensibility of the diffusion NMR technique has been approached in some cases. Despite this limitation, useful information have been obtained. The hydrodynamic dimensions of the diffusing molecular species have been derived from the measured translational self-diffusion coefficient (D_t) through the modified Stokes−Einstein equation (eq 3),[30] which takes into account the ellipsoidal shape of **1** and **3**:

$$D_t = \frac{kT}{f_s c \pi \eta \sqrt[3]{ab^2}} \qquad (3)$$

In eq 3, k is the Boltzmann constant, T is the absolute temperature, η is the fluid viscosity, c is the "size factor", f_s is the "shape factor", and a and b are the major and minor semiaxes of the ellipsoid, respectively. The dependence of f_s on a and b for prolate or oblate ellipsoids is known.[30] The structural parameter P, defined as $kT/\pi\eta D_t = f_s c\sqrt[3]{ab^2}$, has been thus derived from the experimentally measured D_t values (Table 4). Since both f_s and c can be expressed as a function of a and b,[30] we computed the structural parameter P from the calculated DFT optimized structures assuming for **1** and **3** oblate (disklike) ellipsoidal shapes. A major semiaxis a_M (where M stands for a monomeric structure) of the ellipsoid equal to 9.46 Å has been evaluated corresponding to the average distance from the metal center of the terminal *para*-H of the phenyl group (9.4 Å), the terminal NO_2 group (14.1 Å), and the pyrrolic H (4.7 Å) (Figure 7).

The minor semiaxis (b_M) has been set equal to 2.65 Å. As a consequence, the computed value P_M of the structural parameter for both **1** and **3** is 38.2 Å, in excellent agreement with the experimental P value obtained for **3** in $CDCl_3$ at the lowest concentration (38.3 Å, entry 6 in Table 4).

As expected for the lack of formation of a pentacoordinated adduct with pyridine, the experimental value of P_M of **3** at the same concentration but in the presence of excess pyridine does not change (38.4 Å, entry 7 in Table 4). The experimental P value is always higher than the calculated P_M value, in particular for **1**, but also for **3**, although to a lower extent, by increasing concentration. The maximum value of P experimentally obtained for **1** in $CDCl_3$ is 42.3 Å. This is evidence of an associative process for both **1** and **3**.

In order to quantify the level of aggregation, some hypotheses have been proposed about the possible structures of the aggregates.[31] Two possibilities have been taken into account: (1) two monomers perfectly stack minimizing the metal−metal distance; (2) a staggered interaction takes place strengthened by the intermolecular coordination of the NMe_2 donor group of one chromophore to the metal center of another chromophore, leading to a dimeric aggregate of either H or J type (Figure 4). In model 1, the major axis remains unaltered (a_D = 9.46 Å, when D stays for dimer) while the minor axis doubles (b_D = 5.3 Å). In model 2, b_D still doubles (5.3 Å), while a_D increases to 13.9 Å for both H or J aggregation. The calculated P_D values are then 45.3 Å and 63.3 Å for models 1 and 2, respectively. Since the maximum experimental P value is 42.3 Å (see Table 4 in the case of **1**), we can assume that the aggregation process for both **1** and **3** does not proceed beyond dimerization. Starting from the computed values of P_M and P_D, the estimation of the molar fractions of the monomeric (x_M) and dimeric (x_D) species at each concentration and of the dimerization equilibrium constant (K_D) can be evaluated by eq 4, where P is the experimental value (Table 4).

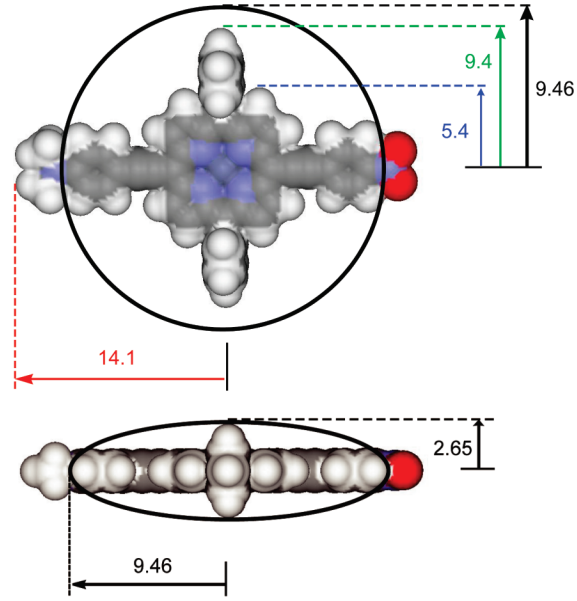

Figure 7. Top and lateral views of the van der Waals surfaces of chromophore **1** or **3**, showing the structural parameters (data are in Å) of the ellipsoid used as geometrical structural model for the analysis of the PGSE NMR experimental data.

$$P = x_M P_M + x_D P_D \qquad (4)$$

The NLO chromophore **1** shows a higher tendency to aggregate than the NLO chromophore **3**. Taking into consideration model 1, a K_D value of 1.75×10^5 M^{-1} ($\Delta G°$(296 K) = −6.4 kcal/mol) can be estimated for **1** (Table 4, entry 1)

with a predominant presence of the dimeric aggregate at a concentration about 10^{-5} M, while for **3** a K_D value of 10^3 M^{-1} ($\Delta G°(296\ K) = -3.7$ kcal/mol) is estimated, a value roughly 2 orders of magnitude smaller (Table 4, entry 8). Taking into consideration model 2, the values of K_D decrease by about 1 order of magnitude for both **1** and **3**, that is from about 10^5 to about 10^4 for **1** ($\Delta G°(296\ K) = -4.8$ kcal/mol) and from 10^3 to about 10^2 for **3** ($\Delta G°(296\ K) = -2.7$ kcal/mol) with a lower tendency to aggregate for **1**, which remains in both cases much higher than that of **3** (Table 4).

Of course due to the low solubility of both **3** and in particular **1**, the above values should be considered as the basis for detecting the main trends, but not as absolute values.

In order to clarify which model is more appropriate for each NLO chromophore, some PGSE NMR measurements have been performed in $CHCl_3$ after addition of an excess of pyridine and also in a more polar but very weak donor solvent such as nitrobenzene. In agreement with the EFISH investigation and with the electronic absorption spectra and theoretical calculations, the addition of excess pyridine to a 3.8×10^{-4} M $CDCl_3$ solution of **3** does not produce any significant variation of the *P* value, as expected for a lack of axial pentacoordination, while it causes a decrease of the *P* value for **1**. The experimental *P* value of **1-py** (39.97 Å, entry 3 in Table 4) is very close to the theoretical *P* value for an axially pentacoordinated pyridine adduct of **1** ($P = 40.7$ Å) computed following the procedure above-described in the case of the monomeric and dimeric structures. Such a relevant effect on the value of *P* by addition of pyridine to a $CHCl_3$ solution of **1** would suggest that its aggregation occurs mainly through coordination of the donor NMe_2 group of one chromophore to the zinc atom of another chromophore (model 2), affording the J type dimeric aggregate described in Figure 4. Another hint to this suggestion comes from the relatively small variation of the aggregation of **1** when dissolved in a more polar solvent such as $C_6H_5NO_2$ that should weaken $\pi-\pi$ stacking interactions but does not interfere with the bonding of the NMe_2 group (entries 4 and 5, Table 4).

The lower tendency of **3** to aggregate (aggregation becomes significant only at concentrations around 5×10^{-4} M, while it is already relevant at concentrations around 3×10^{-5} M for **1**; see Table 4, entries 8 and 1, respectively) is evidence for a very weak interaction of the two porphyrinic chromophores. Such a weak dimerization process may occur by antiparallel (H type) dipolar interactions between the two porphyrinic chromophores due to the significant dipole moment (about 13 D)[9] of **3**. Such antiparallel alignment does not produce a second order NLO response, and therefore, it may explain why the value $\beta_{1.907}$ of **3** decreases by increasing concentration to about 10^{-4} M (Table 2), when a H type weak aggregation starts to take place (entry 8, Table 4).

In conclusion, this PGSE NMR investigation has produced additional evidence that the increase of the second order NLO response of **1** in $CHCl_3$ solution (Table 2) is due to a J aggregation process.

Conclusions

This investigation has shown, by a series of different experimental techniques and by theoretical CP-DFT and CP-HF calculations, that the second order NLO response of [5-[[4′-(Dimethylamino)phenyl]ethynyl]-15-[(4″-nitrophenyl)ethynyl]-10,20-diphenylporphyrinate]M(II) (M = Zn (**1**), Ni (**3**)) chromophores is barely affected by the nature of the metal. However, due to the presence of aggregation processes, which involve the tendency of the Zn(II) metal center to axial coordination, it is dependent on the donor and dipolar properties of the solvent. The metal may play a role in tuning the second order NLO response, but only in a nondonor solvent of low dielectric constant such as $CHCl_3$, which allows aggregation processes.

We have also clearly evidenced, both experimentally and theoretically, the formation in $CHCl_3$ solution of different types of aggregates for **1** and **3**, due to the different tendency of the Zn(II) and Ni(II) to stabilize J aggregation by axial interaction of the metal centers with the NMe_2 donor group.

While the Zn(II) chromophore **1** shows a significant tendency to axially interact with a donor molecule such as pyridine, such axial interaction does not take place in the case of the Ni(II) chromophore **3**.

Since a J dimeric aggregate is stabilized by a donor−acceptor interaction of the NMe_2 group of one chromophore with the Zn(II) center of the other chromophore, such a stabilization is possible for **1** but not for **3**. We have produced EFISH evidence for a different process of aggregation in $CHCl_3$ solution in the case of **3**.

The tendency of chromophores **1** and **3** to form dimers of different stability in $CHCl_3$ solution has been confirmed by the PGSE NMR investigation, which has shown that in $CHCl_3$ a more stable J aggregate is plausible for **1**, while a less stable dimeric aggregate based on H type dipolar interactions is more plausible for **3**.

In summary, the doubling of the EFISH $\beta_{1.907}$ values measured for **1** in $CHCl_3$ solution, with respect to those obtained in $CHCl_3$ solution after addition of excess pyridine or in DMF solution, is due to the stabilization, already in diluted $CHCl_3$ solution, of a certain amount of dimeric J aggregates, while the decrease of the $\beta_{1.907}$ values of **3** by strongly increasing concentration can be due to a small amount of a weak H type aggregate stabilized in an antiparallel arrangement by dipolar interaction of the two chromophores.

Moreover, we have experimentally confirmed the theoretical suggestion[9] that the value of the quadratic hyperpolarizability of the NLO chromophores **1** and **3** is not dependent on the nature of the metal and that its value is about 200×10^{-30} esu, working with an incident wavelength of 1.907 μm. In $CHCl_3$ the higher value of the quadratic hyperpolarizability of **1** up to about 430×10^{-30} esu and the lower value of 3 up to $50-90 \times 10^{-30}$ esu are due to aggregation processes controlled by the nature of the metal center. Interestingly, such values are always much lower than those previously reported for **1** in $CHCl_3$ solution,[3,5] but working with an incident wavelength of 1.067 μm. In this latter case, the second harmonic at about 500 μm is quite close to the very strong B band, and therefore an enhancement of the second order NLO response due to dispersion effects can take place, as suggested by CP-HF calculations.[9]

Therefore, our investigation has evidenced that the nature of the solvent must be carefully taken into account when discussing the second order NLO response of NLO chromophores which can aggregate in a nondonor solvent of low polarity such as $CHCl_3$.

Acknowledgment. This work was supported by the Ministero dell'Istruzione, dell'Università e della Ricerca (FIRB 2003 - Research Title: Molecular compounds and hybrid nanostructured materials with resonant and nonresonant optical properties for photonic devices and PRIN 2007), and by the Consiglio Nazionale delle Ricerche. We thank Dr. S. Righetto for help with EFISH measurements.

References and Notes

(1) (a) Dalton, L. R. In *Handbook of Conducting Polymers*; Skotheim, T. A., Reynolds, J. R., Eds.; CRC Press LLC: Boca Raton, FL, 2007; Chapter 2. (b) Marks, T. J.; Ratner, M. A. *Angew. Chem., Int. Ed. Engl.* **1995**, *34*, 155–173, and references therein. (c) Dalton, L. R.; Steier, W. H.; Robinson, B. H.; Zhang, C.; Ren, A.; Garner, S.; Chen, A.; Londergan, T.; Irwin, L.; Carlson, B.; Fifield, L.; Phelan, G.; Kincaid, C.; Amend, J.; Jen, A. *J. Mater. Chem.* **1999**, *9*, 1905–1920. (d) Characterisation Techniques and Tabulations of Organic Nonlinear Optical Materials; Kuzyk, M. G., Dirk, C. W., Eds.; Marcel Dekker: New York, NY 1998.

(2) (a) Senge, M. O.; Fazekas, M.; Notaras, E. G. A.; Blau, W. J.; Zawadzka, M.; Locos, O. B.; Mhuircheartaigh, E. M. N. *Adv. Mater.* **2007**, *19*, 2737–2774. (b) Kang, H.; Facchetti, A.; Jiang, H.; Cariati, E.; Righetto, S.; Ugo, R.; Zuccaccia, C.; Macchioni, A.; Stern, C. L.; Liu, Z.; Ho, S.-T.; Brown, E. C.; Ratner, M. A.; Marks, T. J. *J. Am. Chem. Soc.* **2007**, *129*, 3267–3286. (c) Coe, B. J. In *Comprehensive Coordination Chemistry II*; McCleverty, J. A., Meyer, T. J., Eds.; Elsevier Pergamon: Oxford, U.K., 2004; Vol. 9, pp 621−687. (d) de la Torre, G.; Vasquez, P.; Agullo-Lopez, F.; Torres, T. *Chem. Rev.* **2004**, *104*, 3723–3750. (e) Abbotto, A.; Beverina, L.; Bradamante, S.; Facchetti, A.; Klein, C.; Pagani, G. A.; Redi-Abshiro, M.; Wortmann, R. *Chem.−Eur. J.* **2003**, *9*, 1991–2007. (f) Jen, A. K.-Y.; Ma, H.; Wu, X.; Wu, J.; Liu, S.; Marder, S. R.; Dalton, L. R.; Shu, C.-F. *SPIE Proc.* **1999**, *112*, 3623–3630.

(3) LeCours, S. M.; Guan, H. W.; DiMagno, S. G.; Wang, C. H.; Therien, M. J. *J. Am. Chem. Soc.* **1996**, *118*, 1497–1503.

(4) (a) Terhune, R. W.; Maker, P. D.; Savage, C. M. *Phys. Rev. Lett.* **1965**, *14*, 681–684. (b) Clays, K.; Persoons, A. *Phys. Rev. Lett.* **1991**, *66*, 2980–2983. (c) Clays, K.; Persoons, A. *Rev. Sci. Instrum.* **1992**, *63*, 3285–3289. (d) Clays, K.; Persoons, A.; De Maeyer, L. In *Modern Nonlinear Optics*; Evans, M., Kielich, S., Eds.; Wiley: New York, 1994; Vol. 3. (e) Hendrickx, E.; Clays, K.; Persoons, A. *Acc. Chem. Res.* **1998**, *31*, 675–683.

(5) Karki, L.; Vance, F. W.; Hupp, J. T.; LeCours, S. M.; Therien, M. J. *J. Am. Chem. Soc.* **1998**, *120*, 2606–2611.

(6) Yeung, M.; Ng, A. C. H.; Drew, M. G. E.; Vorpagel, E.; Breitung, E. M.; McMahon, R. J.; Ng, D. K. P. *J. Org. Chem.* **1998**, *63*, 7143–7150.

(7) Pizzotti, M.; Annoni, E.; Ugo, R.; Bruni, S.; Quici, S.; Fantucci, P.; Bruschi, M.; Zerbi, G.; Del Zoppo, M. *J. Porphyrines Phtalocyanines* **2004**, *8*, 1311–1324.

(8) (a) Levine, B. F.; Bethea, C. G. *Appl. Phys. Lett.* **1974**, *24*, 445–447. (b) Singer, K. D.; Garito, A. F. *J. Chem. Phys.* **1981**, *75*, 3572–3580.

(9) De Angelis, F.; Fantacci, S.; Sgamellotti, A.; Pizzotti, M.; Tessore, F.; Orbelli Biroli, A. *Chem. Phys. Lett.* **2007**, *447*, 10–15.

(10) (a) Schneider, H. J.; Wang, M. *J. Org. Chem.* **1994**, *59*, 7464–7472. (b) Hunter, C. A.; Sander, J. K. M. *J. Am. Chem. Soc.* **1990**, *112*, 5525–5534. (c) Abraham, R. J.; Eivazi, F.; Pearson, H.; Smith, K. M. *Chem. Commun.* **1976**, *69*, 9–701.

(11) (a) Collini, E.; Ferrante, C.; Bozio, R. *J. Phys. Chem. B* **2005**, *109*, 2. (b) Maite, N.; Mazumdar, S.; Periasamy, N. *J. Porpyrins Phtalocyanines* **1998**, *2*, 369–376, and references therein. (c) Zhang, X.; Sasaki, K.; Kuroda, Y. *Bull. Chem. Soc. Jpn.* **2007**, *80*, 536–542.

(12) Bohn, P. W. *Annu. Rev. Phys. Chem.* **1993**, *44*, 37–60.

(13) Shanmugathasan, S.; Johnson, C. K.; Edwards, C.; Matthews, E. K.; Dolphin, D.; Boyle, R. W. J. *J. Porphyrins Phtalocyanines* **2000**, *4*, 228–232.

(14) Ledoux, I.; Zyss, *J. Chem. Phys.* **1982**, *73*, 203–213.

(15) Pizzotti, M.; Ugo, R.; Annoni, E.; Quici, S.; Ledoux-Rak, I.; Zerbi, G.; Dal Zoppo, M.; Fantucci, P. C.; Invernizzi, I. *Inorg. Chim. Acta* **2002**, *340*, 70–80.

(16) Tanner, J. E. *J. Chem. Phys.* **1970**, *52*, 2523–2526.

(17) Mills, R. *J. Phys. Chem.* **1973**, *77*, 685–688. Data at different temperatures were estimated by interpolation of the data reported by Mills, giving DHDO = $1.780 \times 10-9$ m^2 s^{-1} at 295.7 K.

(18) Zuccaccia, D.; Macchioni, A. *Organometallics* **2005**, *24*, 3476–3486.

(19) Frisch, M. J.; Trucks, G. W.; Schlegel, H. B.; Scuseria, G. E.; Robb, M. A.; Cheeseman, J. R.; Montgomery, J. A., Jr.; Vreven, T.; Kudin, K. N.; Burant, J. C.; Millam, J. M.; Iyengar, S. S.; Tomasi, J.; Barone, V.; Mennucci, B.; Cossi, M.; Scalmani, G.; Rega, N.; Petersson, G. A.; Nakatsuji, H.; Hada, M.; Ehara, M.; Toyota, K.; Fukuda, R.; Hasegawa, J.; Ishida, M.; Nakajima, T.; Honda, Y.; Kitao, O.; Nakai, H.; Klene, M.; Li, X.; Knox, J. E.; Hratchian, H. P.; Cross, J. B.; Adamo, C.; Jaramillo, J.; Gomperts, R.; Stratmann, R. E.; Yazyev, O.; Austin, A. J.; Cammi, R.; Pomelli, C.; Ochterski, J. W.; Ayala, P. Y.; Morokuma, K.; Voth, G. A.; Salvador, P.; Dannenberg, J. J.; Zakrzewski, V. G.; Dapprich, S.; Daniels, A. D.; Strain, M. C.; Farkas, O.; Malick, D. K.; Rabuck, A. D.; Raghavachari, K.; Foresman, J. B.; Ortiz, J. V.; Cui, Q.; Baboul, A. G.; Clifford, S.; Cioslowski, J.; Stefanov, B. B.; Liu, G.; Liashenko, A.; Piskorz, P.; Komaromi, I.; Martin, R. L.; Fox, D. J.; Keith, T.; Al-Laham, M. A.; Peng, C. Y.; Nanayakkara, A.; Challacombe, M.; Gill, P. M. W.; Johnson, B.; Chen, W.; Wong, M. W.; Gonzalez, C.; Pople, J. A. Gaussian 03, Revision B.05; Gaussian, Inc.: Pittsburgh, PA, 2003.

(20) Becke, A. D. *J. Chem. Phys.* **1993**, *98*, 5648–5652.

(21) Binkley, J. S.; Pople, J. A.; Hehre, W. J. *J. Am. Chem. Soc.* **1980**, *102*, 939.

(22) Miertus, S.; Scrocco, E.; Tomasi, J. *Chem. Phys.* **1981**, *55*, 117–129.

(23) Cossi, M.; Rega, N.; Scalmani, G.; Barone, V. *J. Comput. Chem.* **2003**, *24*, 669–681.

(24) Cossi, M.; Barone, V. *J. Chem. Phys.* **2001**, *115*, 4708–4717.

(25) Willetts, A.; Rice, J. E.; Burland, D. M.; Shelton, D. P. *J. Chem. Phys.* **1992**, *97*, 7590–7599.

(26) Elangovan, A.; Wang, Y.-H.; Ho, T.-I. *Org. Lett.* **2003**, *5*, 1841–1844.

(27) Ray, P. C.; Leszczynski, J. *Chem. Phys. Lett.* **2006**, *419*, 578–583.

(28) (a) Annoni, E.; Pizzotti, M.; Ugo, R.; Quici, S.; Morotti, T.; Casati, N.; Macchi, P. *Inorg. Chim. Acta* **2006**, *359*, 3029–3041. (b) Nappa, M.; Valentine, J. S. *J. Am. Chem. Soc.* **1978**, *100*, 5075–5080.

(29) Liu, Z. B.; Zhu, Y. Z.; Zhu, Y.; Chen, S. Q.; Zheng, J. Y.; Tian, J. G. *J. Phys. Chem. B* **2006**, *110*, 15140–15145.

(30) Macchioni, A.; Ciancaleoni, G.; Zuccaccia, C.; Zuccaccia, D. *Chem. Soc. Rev.* **2008**, *37*, 479–489, and references therein.

(31) Wang, Y.; Frattarelli, D. L.; Facchetti, A.; Cariati, E.; Tordin, E.; Ugo, R.; Zuccaccia, C.; Macchioni, A.; Wegener, S. L.; Stern, C. L.; Ratner, M. A.; Marks, T. J. *J. Phys. Chem. C* **2008**, *112*, 8005–8015.

JP901919U